HHS Public Access

Author manuscript

Cell Microbiol. Author manuscript; available in PMC 2018 March 01.

Published in final edited form as:

Cell Microbiol. 2017 March ; 19(3): . doi:10.1111/cmi.12668.

Leishmania infection inhibits macrophage motility by altering F-actin dynamics and the expression of adhesion complex proteins

Juliana Perrone Bezerra de Menezes[1,2], **Amrita Koushik**[1], **Satarupa Das**[3], **Can Guven**[3], **Ariel Siegel**[1], **Maria Fernanda Laranjeira-Silva**, **Wolfgang Losert**[3], and **Norma W. Andrews**[1,*]

[1]Department of Cell Biology and Molecular Genetics, University of Maryland, College Park, MD, USA

[2]Laboratório de Patologia e Biointervenção, CPqGM, FIOCRUZ, Rua Waldemar Falcão, 121, Candeal, 40296-710, Salvador, BA, Brazil

[3]Department of Physics, University of Maryland, College Park, MD, USA

Abstract

Leishmania is an intracellular protozoan parasite that causes a broad spectrum of clinical manifestations, ranging from self-healing skin lesions to fatal visceralizing disease. As the host cells of choice for all species of *Leishmania*, macrophages are critical for the establishment of infections. How macrophages contribute to parasite homing to specific tissues and how parasites modulate macrophage function is still poorly understood. In this study we show that *L. amazonensis* infection inhibits macrophage roaming motility. The reduction in macrophage speed is not dependent on particle load or on factors released by infected macrophages. *L. amazonensis*-infected macrophages also show reduced directional migration in response to the chemokine MCP-1. We found that infected macrophages have lower levels of total paxillin, phosphorylated paxillin and phosphorylated FAK when compared to non-infected macrophages, indicating abnormalities in the formation of signaling adhesion complexes that regulate motility. Analysis of the dynamics of actin polymerization at peripheral sites also revealed a markedly enhanced F-actin turnover frequency in *L. amazonensis*-infected macrophages. Thus, *Leishmania* infection inhibits macrophage motility by altering actin dynamics and impairing the expression of proteins that function in plasma membrane-extracellular matrix interactions.

Keywords

motility; migration; macrophage; *Leishmania*

Introduction

Leishmaniasis is a parasitic infection with a broad spectrum of clinical manifestations ranging from self-limiting cutaneous lesions to diffuse cutaneous, mucocutaneous or visceral

*Corresponding author: Norma W. Andrews, Department of Cell Biology and Molecular Genetics, 2134 Bioscience Research Building, University of Maryland, College Park MD 20742-5815, Phone: (301) 405 8418, Fax: (301) 314 9489, andrewsn@umd.edu.

forms, which represent a serious public health challenge. An estimated 12 million people worldwide are currently infected with these parasites, with another 350 million at risk of infection. If untreated, the visceral form of the disease can cause high mortality. Leishmaniasis is initiated by inoculation of *Leishmania* promastigotes into the skin of a susceptible host, during the blood meal of an infected sand fly (Liew *et al.*, 1993). Thereafter, the parasites may remain at the inoculation site or disseminate into other host tissues. Within the mammalian host, *Leishmania* parasites can only survive and replicate intracellularly, and are found predominantly inside acidic parasitophorous vacuoles (PV) of host macrophages (Antoine *et al.*, 1998). The detection of mononuclear phagocytes infected by *Leishmania* in the bloodstream (Liarte *et al.*, 2001) is consistent with the possibility that infected macrophages migrate from the original infection site in the skin, playing a role in dissemination of the disease. However, the mechanisms involved in *Leishmania* dissemination to different host tissues, homing and persistence of infected cells *in vivo* are still poorly understood.

Infection with *Leishmania* has been shown to modulate phagocyte functions associated with cell migration such as signaling, spreading and adhesion to the substrate (Bray *et al.*, 1983; De Almeida *et al.*, 2003; Carvalhal *et al.*, 2004; Pinheiro *et al.*, 2006). Some of these studies suggested that *Leishmania*-induced defects in substrate adhesion might facilitate macrophage migration after infection, promoting parasite dissemination *in vivo* (Carvalhal et al., 2004; Pinheiro et al. 2006; Figueira et al., 2015). However, other authors have reached the opposite conclusion, proposing that infection with *Leishmania* impairs the ability of macrophages to migrate (Bray *et al.*, 1983). In order to clarify this important aspect of the biology of *Leishmania* infections, it is important to consider that cell locomotion involves net protrusion at the front leading edge and retraction at the rear. This process is regulated through the dynamic reorganization of actin microfilaments and tubulin-based microtubules and involves a number of different factors, including modulation of cell adhesion to the substrate (Worthylake *et al.*, 2001; Rafelski *et al.*, 2004).

The initial response of an isolated cell to a migration stimulus is to polarize and extend membrane protrusions, which define the direction of locomotion. These protrusions are formed as a result of actin polymerization and are stabilized by adhesion to the extracellular matrix – facilitated in many cases through integrin receptors that are linked to the actin cytoskeleton (de Fougerolles *et al.*, 2002; Verkhovsky *et al.*, 2003; Huttenlocher *et al.*, 2011). The correct spatial and temporal control of adhesion sites and their disassembly at the leading and trailing edges of cells is critical for efficient cell migration. Thus, modulation of adhesion signaling via integrin receptors and the surrounding extracellular matrix (ECM) plays an essential role in cell motility (Huveneers *et al.*, 2009). Upon integrin engagement, intracellular signaling is initiated through focal adhesion kinase (FAK) and Src family kinases, as well as scaffolding molecules such as talin, vinculin and paxillin. Paxillin is a highly phosphorylated multidomain protein that localizes to focal adhesions through interactions with the cytoplasmic tails of integrins, providing multiple docking sites for an array of signaling and structural proteins. Importantly, paxillin provides a platform for protein tyrosine kinases such as FAK/Pyk2 and Src, which are activated as a result of adhesion or growth factor stimulation. Phosphorylation of paxillin by these activated kinases recruits effector molecules, which transduce external signals into changes in cell motility

(Turner, 2000). Thus, paxillin is a key intracellular plasma membrane-associated molecule that coordinates adhesion signaling molecules, actin polymerization and cell migration (Turner, 2000, Huveneers *et al.*, 2009, Linder *et al.*, 2003). In this study we examined the impact of *Leishmania* infection on macrophage motility, and found that inhibition of this process is associated with reduced expression of paxillin and other components of the focal adhesion signaling complex, and a markedly altered F-actin dynamics in lamellipodia.

Results

Infection with *L. amazonensis* inhibits macrophage motility and migration

To evaluate the impact of *L. amazonensis* on the motility and migration of bone marrow-derived macrophages (BMDM), we analyzed their ability to migrate 6, 24 and 48 h after infection using time-lapse video microscopy. Our real time movies showed that macrophages infected with *L. amazonensis* (identified by RFP expression) migrate less than uninfected macrophages (Fig. 1A and 1B). Reduction in macrophage motility was observed as soon as 24 h after infection, before the onset of parasite replication and full expansion of the parasitophorous vacuoles (PV) (Fig. 1A).

To further examine the migration properties of *L. amazonensis*-infected macrophages, we evaluated their ability to migrate directionally in response to monocyte chemoattractant protein-1 (MCP-1), a key chemokine that regulates migration and infiltration of monocytes and macrophages. Notably, following *L. amazonensis* infection, macrophages migrated significantly less than uninfected macrophages towards the lower compartment of a Boyden chamber containing MCP-1 (Fig. 1C). These findings indicate that *L. amazonensis* intracellular infection interferes with the ability of macrophages to move and directionally migrate.

Inhibition of macrophage motility is not dependent on PV expansion, particle load or factors released from infected cells

The modulation of macrophage motility observed in *L. amazonensis*-infected macrophages might be directly induced by the parasites, or represent an indirect consequence of other factors that interfere with the migration process. To investigate this issue, we evaluated whether the inhibition of macrophage motility induced by *L. amazonensis* was dependent on mechanical load factors, or by molecules released into the medium by infected macrophages. First, we compared the motility of *L. amazonensis*-infected macrophages carrying increasing numbers of parasites. Our results suggest that the reduced macrophage motility caused by infection is not due to parasite load, because no significant difference was observed between macrophages infected with one, three or more parasites (Fig. 2A). Next, we examined if phagocytosis of Zymosan particles (yeast cell wall) affected macrophage motility. The migration speed of macrophages containing or not Zymosan particles was very similar, while infection with *L. amazonensis* under the same conditions showed the expected reduction in motility (Fig. 2B). Zymosan uptake resulted in no reduction in motility even after macrophages were overloaded with the particles, through exposure to high Zymosan/BMDM ratios (results not shown). To verify the influence of possible molecules released into the medium by infected macrophages on macrophage migration, we compared the

motility of infected macrophages in a separate culture (control) with infected and non-infected macrophages present in the same culture. The motility of non-infected macrophages was not altered when they were in the vicinity of infected macrophages (Fig. 2C). These results strongly support the hypothesis that *Leishmania*-induced inhibition of macrophage motility is not dependent solely on particle load, or on soluble factors released from infected cells.

Infection with *L. amazonensis* inhibits expression of adhesion complex proteins

We proceeded to investigate the molecular mechanisms involved in the inhibition of macrophage motility induced by *Leishmania*. Substrate adhesion is an important component of motility, required for cells to propel their leading edge forward (Huveneers *et al.*, 2009). In many cells adhesion induces FAK autophosphorylation on tyrosine 397, which recruits Src to focal adhesions (Schaller *et al.*, 1994). Subsequent Src-mediated phosphorylation of FAK at Y576/577 renders FAK fully active, followed by FAK–Src complex-mediated phosphorylation of multiple scaffolding and signaling proteins at focal adhesions. An important member of the group of FAK-Src-phosphorylated signaling proteins involved in adhesion dynamics and motility is paxillin, an essential focal adhesion-associated adaptor protein (Playford *et al.*, 2004; Mitra *et al.*, 2006; Huttenlocher *et al.*, 2011). In macrophages, substrate adhesion and extracellular matrix remodeling is mediated by podosomes, highly dynamic adhesion structures that share various molecular components with classical focal adhesions, including an intracellular protein complex containing paxillin and FAK family members (Linder *et al.*, 2003). Thus, to investigate adhesion complexes and their potential role in the reduced motility observed after *Leishmania* infection, we determined paxilin and pFAK levels in *L. amazonensis*-infected macrophages. We found that the total level of paxillin protein and the amount of its active, phosphorylated form was markedly decreased in BMDM infected with *L. amazonensis* (Fig. 3A, Fig. 3B and Fig. 3C), and the same was observed with phosphorylated FAK (Fig. 3D). Collectively, our findings indicate that *L. amazonensis* infection disrupts FAK and paxillin-dependent formation of adhesion complexes, providing an explanation for the altered macrophage motility.

Macrophages infected with *L. amazonensis* show altered actin dynamics at the leading edge

An essential step in cell migration is reorganization of the actin cytoskeleton. Thus, we examined whether the reduction in motility observed after *L. amazonensis* infection was associated with alterations in actin filament organization and dynamics, by staining infected BMDM with phalloidin that binds to filamentous actin (F-actin) bundles. The phalloidin staining pattern suggested that zones of active of actin polymerization were present along the whole circumference of *Leishmania*-infected infected macrophages, instead of predominantly at the leading edge as seen in uninfected cells (Fig. 3E). To understand the dynamic changes in actin polymerization underlying this altered F-actin pattern, we performed live time-lapse fluorescence video microscopy of BMDM isolated from Lifeact mice, which express the 17 amino acid peptide Lifeact fused to EGFP (Riedl *et al.*, 2010), after infection with with RFP-expressing *L. amazonensis* amastigotes. In uninfected macrophages the videos revealed the expected localization of F-actin dynamics to sites of vigorous membrane ruffling, at leading edge protrusions (video S1, Fig. 4 Control). Infected

BMDM, in contrast, showed a significantly less polarized pattern of actin polymerization, with undefined leading edges and a form of oscillating F-actin dynamics on the cell boundaries that was distributed to multiple regions around the whole circumference of *L. amazonensis*-containing macrophages (video S2, Fig. 4 *L. amazonensis*). Image analysis was performed to examine actin-filament turnover rates on lamelipodia formed at the periphery of infected or non-infected BMDM. Kymograph analysis revealed a markedly altered pattern of multiple actin polymerization regions that alternate in location in infected BMDM, in contrast to the steady, propagating actin polymerization waves formed at the leading edge of uninfected, migrating control macrophages (Fig. 5A). Shape analysis showed significantly more circular actin polymerization features in *L. amazonensis*-infected macrophages, versus excentric actin polymerization features, located along the membrane, in control macrophages (Fig. 5B,C). These results indicate that mouse macrophages infected with *L. amazonensis* have a significantly higher frequency of formation and turnover of the F-actin cytoskeleton when compared to non-infected macrophages.

Discussion

Using time-lapse video microscopy and image analysis as major experimental tools, we found that infection with *Leishmania amazonensis* parasites reduces the motility of mouse macrophages, during random roaming and also directional migration driven by chemotaxis. Investigating the molecular mechanisms responsible for this effect, our study revealed a significant parasite-induced reduction in phosphorylated FAK and paxilin, components of key adhesion signaling complexes that control the ability of migrating cells to form adequate substrate anchorage, which is often important for propulsion of the leading edge (Huttenlocher *et al.*, 2011; Blanchoin *et al.*, 2014). These changes were associated with marked changes in the dynamics of F-actin waves on lamelipodia, which we defined through quantitative analysis of shape dynamics.

Although the underlying molecular mechanisms involved were not elucidated, an earlier study reported reduced migration of macrophages infected with *L. mexicana mexicana*, in good agreement with our results using *L. amazonensis* (Bray *et al.*, 1983). That study reported no changes in phagocytosis or lysosomal enzyme secretion in response to stimuli, but interestingly found that infection enhanced macrophage pinocytosis and bactericidal ability (Bray *et al.*, 1983). Also consistent with our findings, *L. amazonensis* infection was reported to reduce the adherence of mouse peritoneal macrophages or human peripheral blood monocytes to inflamed connective tissue (Carvalhal *et al.*, 2004, Pinheiro *et al.*, 2006). In a careful quantitative study, the same laboratory examined the effect of infection with *L. amazonensis* on the spreading of human monocytes on fibronectin-coated surfaces mediated by VLA-4, a β1 integrin involved in leukocyte adhesion to fibronectin, and found that infection shifted the median spreading area from 72 μm^2 to just 41 μm^2 (Figueira *et al.*, 2015). Although macrophage motility was not examined in those studies, the authors suggested that the observed reduced substrate adherence could result in enhanced migration of the host cells, influencing parasite dissemination *in vivo*. Our study suggests that *L. amazonensis* infection may actually impair the ability of macrophages to leave sites of infection, consistent with the cutaneous and predominantly localized pattern of *L. amazonensis* lesions (McMahon-Pratt *et al.*, 2004). Reduced migration of infected dendritic

cells is also likely to have an important impact on immune responses to *Leishmania*, and this possibility is emphasized by a recent study showing that *L. amazonensis* infection inhibits the migration of dendritic cells from inflammatory sites to draining lymph nodes (Hermida *et al.*, 2014).

Actin polymerization alone is known to generate forces that are sufficient to drive protrusions at the leading edge of migrating cells (Mitchison *et al.*, 1996, Prass *et al.*, 2006, Keren *et al.*, 2008, Rottner *et al.*, 2011). The role of cortical actin dynamics in cell migration on flat substrates has been a subject of intense investigation (Blanchoin *et al.*, 2014), and recent studies found that fluorescent signals from the plasma membrane and the F-actin cortical cytoskeleton are highly correlated in all stages of cell protrusion and actin wave propagation (Kapustina *et al.*, 2013, Driscoll *et al.*, 2015). Our data showing reduction in the phosphorylated forms of FAK and paxilin suggest that *L. amazonensis* infection may impair the formation of adhesion signaling complexes at focal adhesions/podosomes on the plasma membrane, an effect likely to influence the dynamic changes that we observed in the cortical actin cytoskeleton (Gardel *et al.*, 2010). Although additional studies are needed to strengthen this hypothesis, *Leishmania*-mediated impairement of adhesion complexes is supported by prior studies that specifically examined the substrate adhesion properties of mouse and human macrophages, and detected a marked inhibition after infection with *L. amazonensis* (Cervalhal *et al.*, 2004, Figueira *et al.* 2015). Thus, with this study we advance the current understanding of the molecular mechanism underlying the reduced motility of *Leishmania*-infected macrophages, paving the way for future identification of the parasite factors that mediate this process.

Materials and Methods

Ethics statement

All animal work was conducted according to the National Institutes of Health guidelines for the housing and care of laboratory animals and performed under protocol # R-11-73 approved by the University of Maryland College Park Institutional Animal Care and Use Committee. The University of Maryland at College Park is a fully AAALAC-accredited institution.

Leishmania parasites

Wild type *Leishmania amazonensis* (IFLA/BR/67/PH8 strain, expressing or not RFP) promastigotes were maintained *in vitro* at 26°C in M199 (Invitrogen), 40 mm HEPES, pH 7.4, 20% heat-inactivated FBS, 5% penicillin/streptomycin, 0.1% hemin (from a 25 mg/ml stock in 50% triethanolamine), 10 mm adenine, and 5 mm l-glutamine. To obtain *L. amazonensis* axenic amastigotes, stationary phase cultures rich in metacyclic promastigotes were incubated at 32°C in acidified media, as previously described (Flannery *et al.*, 2011), resuspended in BMDM medium and added to BMDM at a MOI = 5.

Mouse Bone Marrow Macrophages (BMDM)

BMDM obtained from WT C57Bl/6 mice (The Jackson Laboratory) or Lifeact C57Bl/6 mice (expressing the 17 amino acid peptide Lifeact that specifically labels F-actin fused to

EGFP (Riedl *et al.*, 2010)) were cultured in RPMI 1640 containing 20% heat-inactivated endotoxin-free FBS, 100 units/ml penicillin and 100 μg/ml streptomycin and 50 ng/ml human Recombinant M-CSF (Peprotech). Mature, adherent BMDM were detached from dishes with PBS/1 mM EDTA, viability was determined with a trypan-blue exclusion test and incubated overnight at 37°C in a 5% CO2 incubator prior to use in experiments.

BMDM infection

A total of 2 $\times 10^5$ BMDMs were plated on Mattek dishes for motility experiments 24 h prior to experiments, and on transwell plates for migration assays, 5 h prior to experiments. To obtain protein extracts and for immunofluorescence assays, a total of 2 $\times 10^6$ BMDMs per well were plated on a 6 well plate 24 h prior to experiments. *L. amazonensis* axenic amastigotes were added to BMDM for 1 h at 34°C at a MOI = 5, washed in PBS to remove non-internalized parasites and reincubated for 24 or 48 h at 34°C, for the motility experiments and for western blot experiments. For *L. amazonensis* and *L. donovani* metacyclic promastigotes infection, parasites were added to BMDM for 3 h at 34°C at a MOI = 5, washed in PBS to remove non-internalized parasites and reincubated for 24, 48 or 72 h at 34°C.

Zymosan phagocytosis

BMDMs plated as described above were incubated with Zymosan A from *Saccharomyces cerevisiae* (Sigma-Aldrich) at a ratio of 5,10 and 20 particles per BMDM for 1 h at 34°C, washed in PBS to remove non-internalized particles and reincubated for 48 h prior to the motility analysis.

Cell motility

Time lapse imaging of macrophages infected with *L. amazonensis* axenic amastigotes or *L. amazonensis* or *L. donovani* metacyclic promastigotes and non-infected macrophages was carried out using an UltraView Vox spinning disk confocal system (Perkin Elmer) equipped with an incubation chamber where cells were kept at 37°C in 5% CO_2 atmosphere. Phase-contrast time-lapse images were acquired every min for 1 h using a 10× objective lens. Movements of individual cells were traced on the acquired digital images by tracking the position of cell nuclei using Volocity software. The velocity of each cell was calculated using Volocity software and results expressed as the mean of at least 10 cells per group.

Macrophage migration

Chemotaxis was assayed in Boyden chambers with polycarbonate membranes (12 well, 5-μm pores, Corning® Transwell® polycarbonate membrane cell culture inserts). Macrophages were starved in serum-free RPMI 1640 medium overnight and then seeded at a concentration of 2 × 10^5 macrophages per transwell insert in serum-free RPMI 1640 medium. After 1 h of incubation at 37°C, macrophages were infected with *L. amazonensis* axenic amastigotes for 1 h, washed and allowed to migrate toward RPMI containing 100ng/ml MCP-1 in the lower compartment for 5 h. The membranes were washed three times with PBS, fixed with 4% paraformaldehyde for 10 min, washed twice with PBS and incubated with 10 mg/ml DAPI for nuclear staining. The upper side of the filter was

scrapped to remove residual non-migrating macrophages. Fifteen random fields were counted per well on the bottom side of the filter using a fluorescence microscope. The number of uninfected macrophages migrating to the lower chamber was compared with that of macrophages infected with *L. amazonensis* axenic amastigotes.

Immunofluorescence

Macrophages infected or not with *L. amazonensis* axenic amastigotes were fixed with 4% paraformaldehyde for 15 min, washed with PBS 3 times and quenched with 15 mM NH_4Cl for 20 min. Coverslips were washed 3 times with PBS, incubated in blocking solution (3% bovine serum albumin [BSA] in PBS) for 1 h, washed 3 times with PBS, permeabilized with 0.15% saponin-PBS for 15 min and incubated with 1:200 rabbit anti-paxillin (pY^{118}) (Invitrogen) or 1:500 anti-Lamp1 hybridoma supernantant (1D4B, Developmental Studies Hybridoma Bank) diluted in PBS 1% BSA 0.15% saponin for 1 h. This was followed by incubation with anti-rabbit or anti-rat IgG Alexa Fluor 488 for 1 h, 10 mg/ml DAPI for nuclear staining, and mounting with ProLong Gold antifade reagent (Invitrogen). Secondary antibodies were purchased from Molecular Probes. Images were acquired through a Leica SPX5 confocal microscope using a 63×/1.4 objective and processed using Volocity Software (PerkinElmer).

Protein extraction and Western Blot

Macrophages infected or not with *L. amazonensis* axenic amastigotes were washed twice with cold PBS, scraped from the dish, collected by centrifugation (335 *g*) for 10 min at 4°C, lysed in 30 μl RIPA buffer (50 mM Tris-HCl, pH 8.0, 150 mM NaCl, 1% Nonidet P-40, 0.50% sodium deoxycholate, 0.10% SDS) with protease inhibitors (Roche), and centrifuged at 14000 g for 15 min at 4°C to remove insoluble material. Lysates were assayed for protein content (Pierce BSA Protein Assay kit), 60 μg per sample were mixed with SDS sample buffer at room temperature for 30 min, separated by SDS-PAGE (without sample boiling) and transferred to a PVDF membrane (Millipore). Membranes were incubated overnight with 1:10000 mouse anti-paxillin antibody (BD Transduction Laboratories), 1:1000 rabbit anti-paxillin (pY^{118}) (Invitrogen), 1:1000 rabbit anti-FAK (pY^{397}) (Abcam) or 1:5000 anti-actin (Sigma-Aldrich) in blocking buffer (PBS 3% milk, 0.1% Tween), followed by HRP-coupled anti-rabbit IgG or anti mouse IgG secondary antibodies (Amersham Biosciences). Blots were developed using Immun-Star HRP Luminol Enhancer and peroxidase buffer (Bio-Rad) and detected with a Fuji LAS-3000 Imaging System and Image Reader LAS-3000 software. Digital quantifications of chemiluminescence were performed using Image J software.

Actin dynamics videos, kymograph analysis and shape dynamics analysis

Time lapse imaging of Lifeact C57Bl/6 mouse macrophages infected or not with *L. amazonensis* axenic amastigotes was carried out using an UltraView Vox spinning disk confocal system (Perkin Elmer) equipped with an incubator chamber to maintain constant temperature and CO_2 levels. Fluorescence images were acquired every 15 seconds for 30 min using a 60× objective lens. The actin wave propagation speed in infected and control macrophages was measured using space/time plots (Driscoll *et al.*, 2014, Driscoll *et al.*, 2015). Actin waves near the lamellipodia were cropped and resized into a single-pixel width

using ImageJ software (NIH). The same processing was repeated on every cropped image in the time-lapse series. The resized actin waves were also montaged into a space/time plot. Actin-wave propagation speed was obtained by dividing the distance that the wave front traveled by the time lapse. The circularity and the line shape features were quantified using the Matlab function Region Props to obtain area and perimeter values, and the circularity formula 4*pi*area/(perimeter)^2. Probability density function was then computed in order to show the relative strength of the circularity feature that is observed in the infected cells. The box plot was assembled from data of several different cells (n = 25).

Statistical analysis

Data were analyzed by two-tailed Student's *t* test using GraphPad Prism software. A result was considered significant at a *p* value of <0.05.

Supplementary Material

Refer to Web version on PubMed Central for supplementary material.

Acknowledgments

We thank A. Beaven (University of Maryland) and the Department of Cell Biology and Molecular Genetics Imaging Core for assistance with confocal microscopy, Drs. W. Song and H. Miller (U. Maryland) for Lifeact mice, Dr. Matthias Corrotte for help with video assembly, and members of the Andrews laboratory for helpful discussions. This work was supported by National Institutes of Health grant R01 AI67979 to NWA. WL and SD were supported by National Institutes of Health grant R01 GM085574. JPBN was supported by a Ciências sem Fronteiras fellowship (CNPq).

References

Antoine JC, Prina E, Lang T, Courret N. The biogenesis and properties of the parasitophorous vacuoles that harbour Leishmania in murine macrophages. Trends Microbiol. 1998; 6:392–401. [PubMed: 9807783]

Blanchoin L, Boujemaa-Paterski R, Sykes C, Plastino J. Actin dynamics, architecture, and mechanics in cell motility. Physiol Rev. 2014; 94:235–263. [PubMed: 24382887]

Bray RS, Heikal B, Kaye PM, Bray MA. The effect of parasitization by Leishmania mexicana mexicana on macrophage function in vitro. Acta tropica. 1983; 40:29–38. [PubMed: 6134450]

Carvalhal DG, Barbosa A Jr, D'El-Rei Hermida M, Clarencio J, Pinheiro NF Jr, Veras PS, dos-Santos WL. The modelling of mononuclear phagocyte-connective tissue adhesion in vitro: application to disclose a specific inhibitory effect of Leishmania infection. Exp Parasitol. 2004; 107:189–199. [PubMed: 15363945]

De Almeida MC, Cardoso SA, Barral-Netto M. Leishmania (Leishmania) chagasi infection alters the expression of cell adhesion and costimulatory molecules on human monocyte and macrophage. Int J Parasitol. 2003; 33:153–162. [PubMed: 12633653]

de Fougerolles AR, Koteliansky VE. Regulation of monocyte gene expression by the extracellular matrix and its functional implications. Immunological reviews. 2002; 186:208–220. [PubMed: 12234373]

Driscoll MK, Losert W, Jacobson K, Kapustina M. Spatiotemporal relationships between the cell shape and the actomyosin cortex of periodically protruding cells. Cytoskeleton. 2015; 72:268–281. [PubMed: 26147497]

Driscoll MK, Sun X, Guven C, Fourkas JT, Losert W. Cellular contact guidance through dynamic sensing of nanotopography. ACS nano. 2014; 8:3546–3555. [PubMed: 24649900]

Figueira CP, Carvalhal DG, Almeida RA, Hermida M, Touchard D, Robert P, et al. Leishmania infection modulates beta-1 integrin activation and alters the kinetics of monocyte spreading over fibronectin. Sci Rep. 2015; 5:12862. [PubMed: 26249106]

Flannery AR, Huynh C, Mittra B, Mortara RA, Andrews NW. LFR1 ferric iron reductase of Leishmania amazonensis is essential for the generation of infective parasite forms. J Biol Chem. 2011; 286:23266–23279. [PubMed: 21558274]

Gardel ML, Schneider IC, Aratyn-Schaus Y, Waterman CM. Mechanical integration of actin and adhesion dynamics in cell migration. Annu Rev Cell Dev Biol. 2010; 26:315–333. [PubMed: 19575647]

Hermida MD, Doria PG, Taguchi AM, Mengel JO, dos-Santos W. Leishmania amazonensis infection impairs dendritic cell migration from the inflammatory site to the draining lymph node. BMC infectious diseases. 2014; 14:450. [PubMed: 25142021]

Huttenlocher A, Horwitz AR. Integrins in cell migration. Cold Spring Harb Perspect Biol. 2011; 3:a005074. [PubMed: 21885598]

Huveneers S, Danen EH. Adhesion signaling - crosstalk between integrins, Src and Rho. J Cell Sci. 2009; 122:1059–1069. [PubMed: 19339545]

Kapustina M, Elston TC, Jacobson K. Compression and dilation of the membrane-cortex layer generates rapid changes in cell shape. J Cell Biol. 2013; 200:95–108. [PubMed: 23295349]

Keren K, Pincus Z, Allen GM, Barnhart EL, Marriott G, Mogilner A, Theriot JA. Mechanism of shape determination in motile cells. Nature. 2008; 453:475–480. [PubMed: 18497816]

Liarte DB, Mendonca IL, Luz FC, Abreu EA, Mello GW, Farias TJ, et al. QBC for the diagnosis of human and canine american visceral leishmaniasis: preliminary data. Revista da Sociedade Brasileira de Medicina Tropical. 2001; 34:577–581. [PubMed: 11813066]

Liew FY, O'Donnell CA. Immunology of leishmaniasis. Adv Parasitol. 1993; 32:161–259. [PubMed: 8237615]

Linder S, Aepfelbacher M. Podosomes: adhesion hot-spots of invasive cells. Trends Cell Biol. 2003; 13:376–385. [PubMed: 12837608]

McMahon-Pratt D, Alexander J. Does the Leishmania major paradigm of pathogenesis and protection hold for New World cutaneous leishmaniases or the visceral disease? Immunological reviews. 2004; 201:206–224. [PubMed: 15361243]

Mitchison TJ, Cramer LP. Actin-based cell motility and cell locomotion. Cell. 1996; 84:371–379. [PubMed: 8608590]

Mitra SK, Schlaepfer DD. Integrin-regulated FAK-Src signaling in normal and cancer cells. Curr Opin Cell Biol. 2006; 18:516–523. [PubMed: 16919435]

Pinheiro NF Jr, Hermida MD, Macedo MP, Mengel J, Bafica A, dos-Santos WL. Leishmania infection impairs beta 1-integrin function and chemokine receptor expression in mononuclear phagocytes. Infect Immun. 2006; 74:3912–3921. [PubMed: 16790764]

Playford MP, Schaller MD. The interplay between Src and integrins in normal and tumor biology. Oncogene. 2004; 23:7928–7946. [PubMed: 15489911]

Prass M, Jacobson K, Mogilner A, Radmacher M. Direct measurement of the lamellipodial protrusive force in a migrating cell. J Cell Biol. 2006; 174:767–772. [PubMed: 16966418]

Rafelski SM, Theriot JA. Crawling toward a unified model of cell mobility: spatial and temporal regulation of actin dynamics. Annual review of biochemistry. 2004; 73:209–239.

Riedl J, Flynn KC, Raducanu A, Gartner F, Beck G, Bosl M, et al. Lifeact mice for studying F-actin dynamics. Nat Methods. 2010; 7:168–169. [PubMed: 20195247]

Rottner K, Stradal TE. Actin dynamics and turnover in cell motility. Curr Opin Cell Biol. 2011; 23:569–578. [PubMed: 21807492]

Schaller MD, Hildebrand JD, Shannon JD, Fox JW, Vines RR, Parsons JT. Autophosphorylation of the focal adhesion kinase, pp125FAK, directs SH2-dependent binding of pp60src. Molecular and cellular biology. 1994; 14:1680–1688. [PubMed: 7509446]

Turner CE. Paxillin interactions. J Cell Sci. 2000; 113(Pt 23):4139–4140. [PubMed: 11069756]

Verkhovsky AB, Chaga OY, Schaub S, Svitkina TM, Meister JJ, Borisy GG. Orientational order of the lamellipodial actin network as demonstrated in living motile cells. Mol Biol Cell. 2003; 14:4667–4675. [PubMed: 13679520]

Worthylake RA, Burridge K. Leukocyte transendothelial migration: orchestrating the underlying molecular machinery. Curr Opin Cell Biol. 2001; 13:569–577. [PubMed: 11544025]

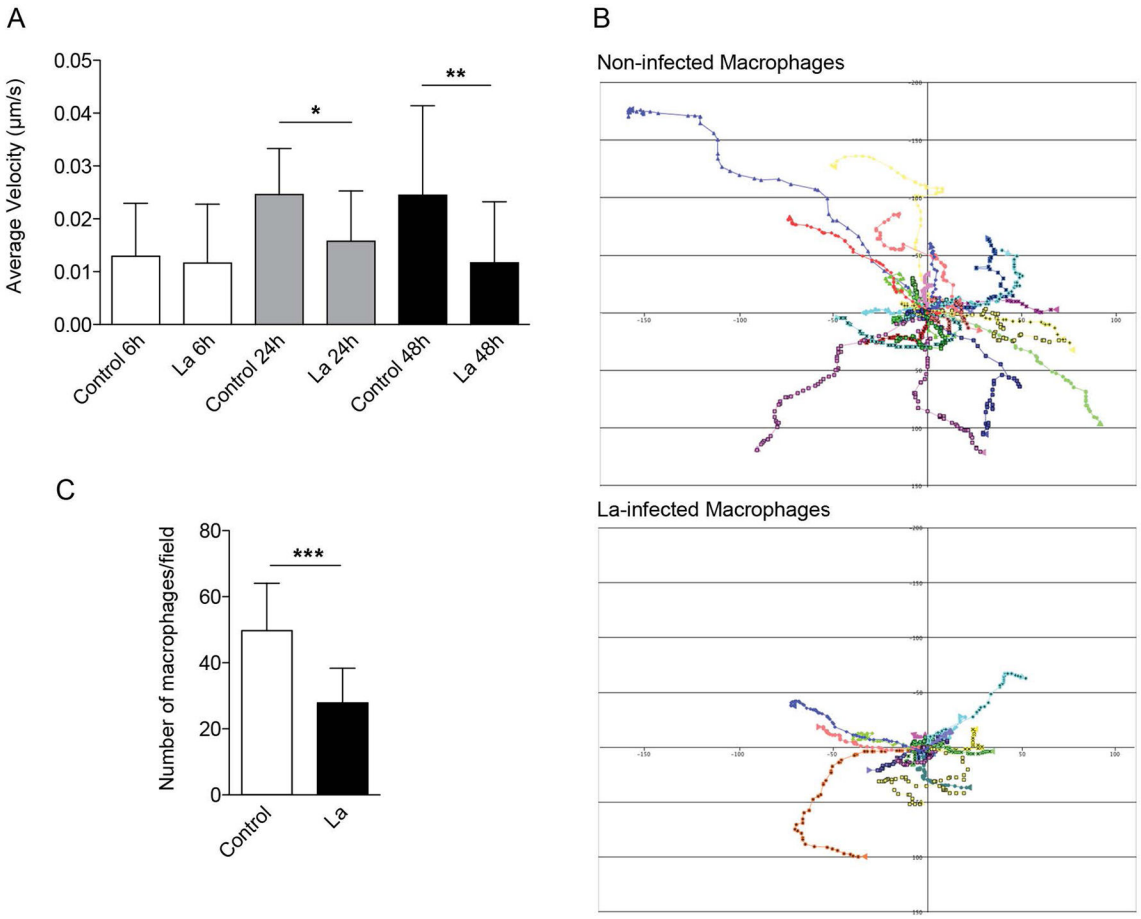

Figure 1. *L. amazonensis* infection inhibits macrophage migration

BMDM were infected (La) or not (control) with *L. amazonensis* axenic amastigotes for 1h. BMDM were then washed to remove extracellular parasites, cultured at 34°C for another 6, 24 or 48 h and assayed for their ability to migrate. For the Boyden chamber chemotaxis migration assays, macrophages were cultured at 34°C for another 5 h. (A) Effect of *L. amazonensis* infection in the migration velocity of macrophages, measured by phase-contrast time-lapse imaging. The data are representative of nine independent experiments. (B) Tracks representing the migration of individual macrophages, non-infected or infected for 48 h, derived from stacks of confocal images acquired every min for 1 h. The results of nine independent experiments are shown for each condition. (C) Effect of *L. amazonensis* infection in macrophage migration through a Boyden chamber membrane containing MCP-1 in the lower chamber. The data are representative of three independent experiments. * $p < 0.05$, ** $p < 0.01$, ** $p < 0.001$ (Student's *t* test) compared with non-infected control (C).

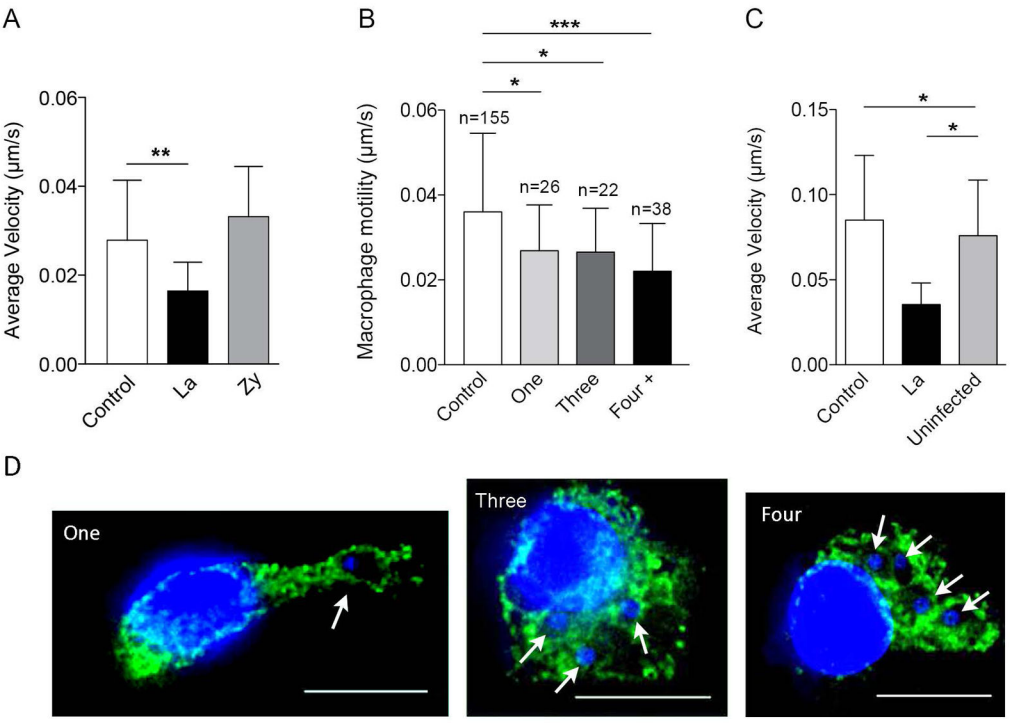

Figure 2. Inhibition of macrophage motility induced by *L. amazonensis* is not dependent on PV expansion, parasite load or secreted factors

BMDM were exposed or not to *L. amazonensis* axenic amastigotes or to Zymosan particles for 1 h. BMDM were washed to remove extracellular parasites or particles, cultured at 34°C for another 24 or 48 h and assayed for their ability to migrate using phase-contrast time-lapse imaging. (A) Velocity of macrophages infected with *L. amazonensis* axenic amastigotes for 48 h carrying one, three, or more parasites. Data are representative of eight independent experiments. (B) Velocity of macrophages 48 h after internalization of *L. amazonensis* (La) or Zymosan particles (Zy). *L. donovani* (Ld), 48 h after infection. Data are representative of three independent experiments. (C) Effect of factors released into the medium by BMDM infected with *L. amazonensis* axenic amastigotes on macrophage motility 24 h after infection. Macrophage velocity was determined in non-infected macrophages in a separate culture (control) and in *L. amazonensis*-infected (La) and non-infected macrophages (uninfected) in the same culture. Data are representative of two independent experiments. (D) Images illustrating macrophages infected with one, three or four *L. amazonensis* axenic amastigotes for 48 h. Green, anti-Lamp1 antibodies; blue, DAPI DNA stain. Bars: 11 µm. * $p < 0.05$, ** $p < 0.01$, ** $p < 0.001$ (Student's *t* test) compared with non-infected control BMDM.

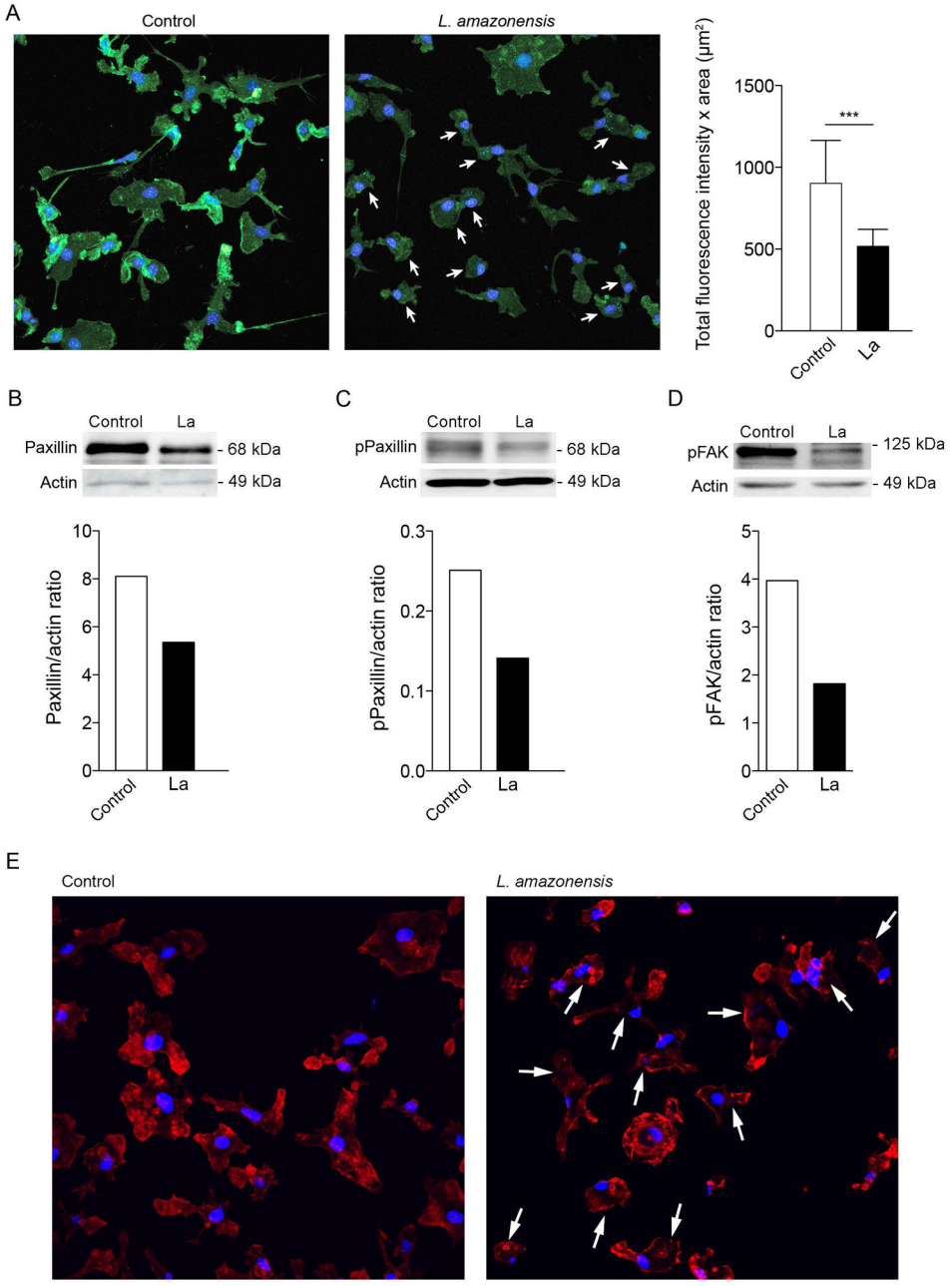

Figure 3. Infection with *L. amazonensis* disrupts paxillin-dependent adhesion complex formation

(A) Effect of *L. amazonensis* infection on phosphorylated paxillin protein levels. BMDM were infected or not with *L. amazonensis* axenic amastigotes for 1 h. BMDM were washed to remove extracellular parasites, cultured at 34°C for another 24 h, fixed and stained with anti-phosphorylated paxillin antibodies. The arrows point to *L. amazonensis*-infected BMDM. On the right is shown the fluorescence intensity from 40 cells for each group quantified using Volocity software. ***, $p < 0.001$ (Student's *t* test) compared with non-infected control. Bar: 30 µm. (B) Effect of *L. amazonensis* infection on total paxillin protein levels. BMDM were infected or not with axenic *L. amazonensis* amastigotes (La) for 1 h,

washed and cultured at 34°C for another 24 h, followed by quantification of total paxillin by Western Blot. Anti-actin antibodies were used as loading controls. Phospho-paxillin/actin ratios were determined by densitometry. (C) Effect of *L. amazonensis* infection on phosphorylated paxillin protein levels. BMDM were infected or not with axenic *L. amazonensis* amastigotes (La) for 1 h, washed and cultured at 34°C for another 24 h, followed by quantification by Western Blot with anti-phospho-paxillin antibodies. Anti-actin antibodies were used as loading controls. Phospho-paxillin/actin ratios were determined by densitometry. (D) Effect of *L. amazonensis* infection on phosphorylated FAK protein levels. BMDM were infected or not with axenic *L. amazonensis* amastigotes (La) for 1 h, washed and cultured at 34°C for another 24 h, followed by quantification by Western Blot with anti-phospho-FAK antibodies. Anti-actin antibodies were used as loading controls. Phospho-FAK/actin ratios were determined by densitometry. The results shown in A–D are representative of three independent experiments. (E) BMDM were infected or not with axenic *L. amazonensis* amastigotes (La) for 1 h, washed and cultured at 34°C for another 24 h, followed by staining with phalloidin. The arrows point to *L. amazonensis*-infected BMDM. The images shown are representative of two independent experiments.

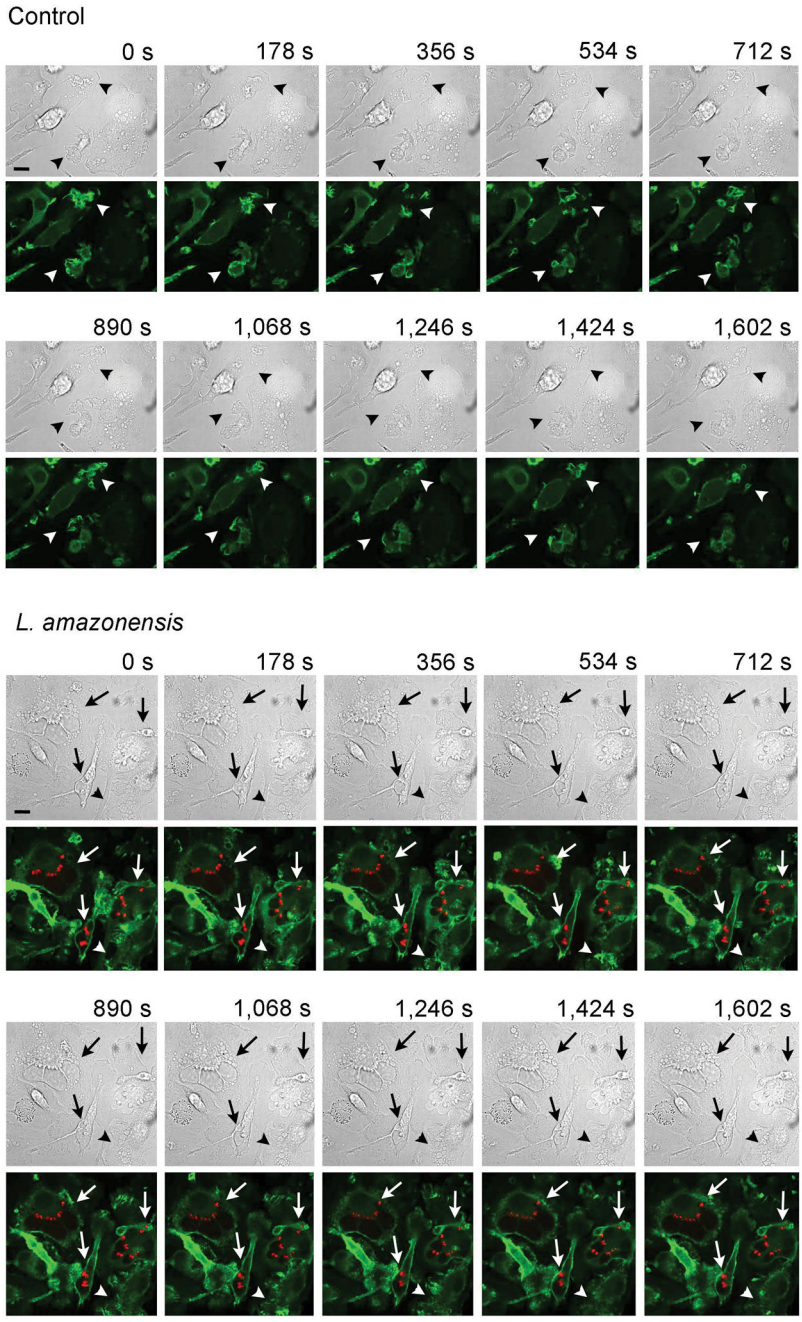

Figure 4. Differential actin filament dynamics during migration of macrophages infected with *L. amazonensis*

BMDM from Lifeact mice were infected or not (control) with *L. amazonensis* axenic amastigotes for 1h. BMDM were then washed to remove extracellular parasites, cultured at 34°C for another 24 h, followed by fluorescence time-lapse image acquisition for 26.7 min. Arrowheads: F-actin (green) dynamics at ruffling leading edges of macrophages. Arrows: infected macrophages showing altered F-actin propagating waves at cell boundaries. Bars: 10 μm. See supplemental videos.

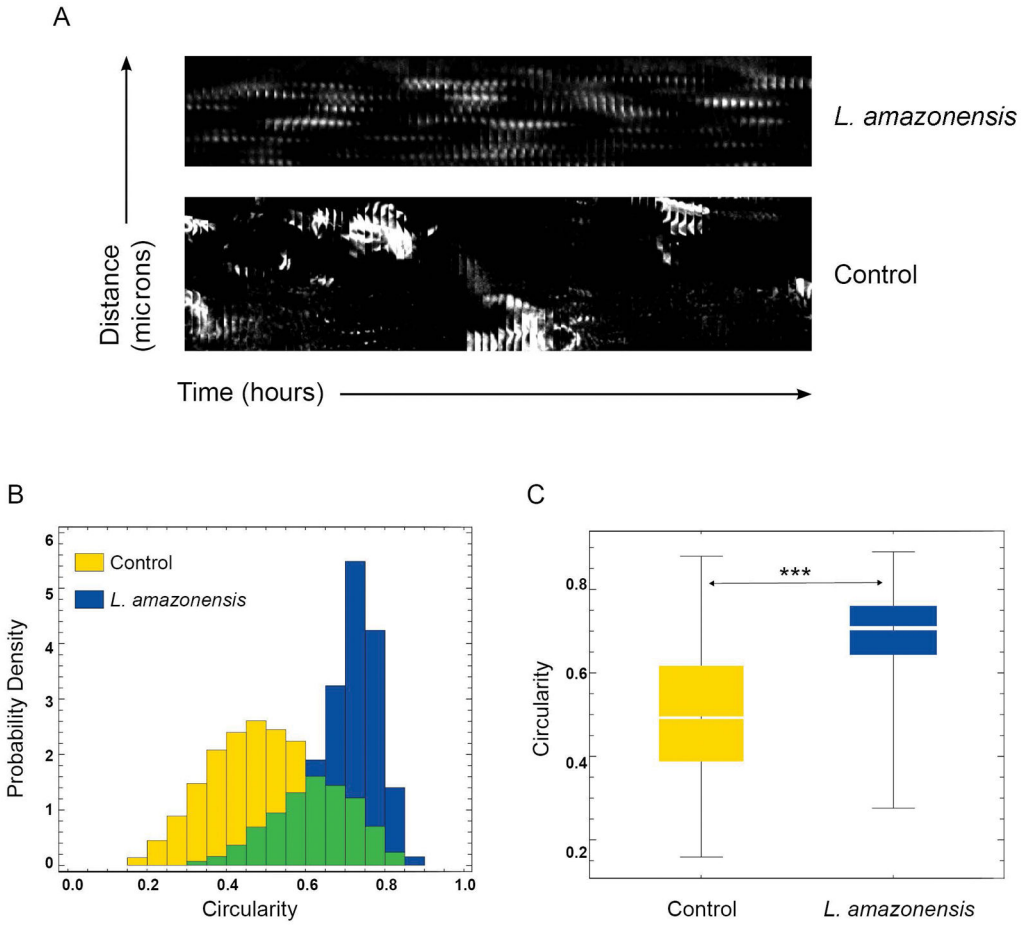

Figure 5. Actin filament dynamic properties are markedly altered in macrophages infected with *L. amazonensis*

BMDM from Lifeact mice were infected or not with *L. amazonensis* axenic amastigotes for 1 h. BMDM were then washed to remove extracellular parasites, cultured at 34°C for another 24 h, followed by fluorescence time-lapse image acquisition. (A) Space/time plot of an actin propagating wave at the lamellipodia front over 200 frames indicating oscillating dotted actin polymerization waves in infected macrophages versus a propagating steady membrane wave front in an actively migrating control macrophage. The results shown are representative of four non-infected macrophages and five infected individual macrophages analyzed. (B) Shape dynamic analysis showing circular actin shape-like features in 25 infected macrophages versus line-like steady actin membranous features in 25 control macrophages. (C) Statistical analysis of the data in (B) indicating that infected macrophages show significantly more circular shape features compared to control macrophages. The boxes show the 50% confidence region from the median (black line). The bars cover a region with 99% confidence level from the median. *** $p<0.01$, $n=25$. The results shown are representative of two independent experiments.